Turk J Phy
24 (2000) , 157 – 169.

Two-Photon Absorption in Size-Quantized Semiconductors with Degenerated Valence Band

T. G. ISMAILOV, M. A. BAGIROV* & B. ÜNAL
Department of Engineering Physics, Faculty of Science,
Ankara University, Tandoğan, 06100 Ankara-TURKEY

Received 07.07.1999

Abstract

Two photon absorption in size-quantized films of semiconductors with degenerated band structures are investigated. The carrier energy spectrum and wavefunctions in the bands are calculated using two-band Kane model with spin taken into accont. Two-photon absorption coefficients for different polarizations of incident radiations are calculated. The strong dependence of two-photon absorption on polarizations are stated.

1. Introduction

Superlattices and other structures with quantum wells are currently the most intensively studied objects of semiconductor electronics. Recent achievements in study and practical applications of two dimensional electron gas (2DEG) constructed from III-V compounds, mainly on the basis of GaAs [1-3] thin films, heterostructures, structure of superlattices among others, have stimulated the search for developing new semiconductor structures such as quantum wires and quantum dots [3-5]. Aside from the traditional III-V compounds, semiconductors such as HgCdTe, HgMnTe, CdMnTe etc., which have unique properties, have been employed to obtain 2DEG materials.

On the basis of such compounds and by changing their composition, one can obtain superlattices of types I, II and III as identified by generally accepted classification [3].

In the present work we consider two-photon absorption of light (TPA) in size quantized films formed from the above mentioned semiconductor type. Desire to investigate TPA in semiconductors stems from the wide possibilities this method may bring [6-9]. First, TPA allows to obtain bulk excitation of semiconductor, which in turn facilitates a study

*Permanent adress: Institute of Physics, Academy of Sciences, 370143, Baku- AZERBAIJAN

volume that is little distorted by the surface. Second, by the help of two photon pumping it is easier to create population inversion in uniform semiconductors and semiconductor structures. Thirdly, since in crystals with inversion symmetry two-photon transitions are allowed between states of the same parity (dipole transitions), using TPA one can observe those energetic states which otherwise cannot be detected in one photon spectra. TPA essentially depends on electric field polarizations that differ drastically from the one photon polarizations. Moreover, TPA depends on polarization even in an isotropic media. It follows from above discussions that TPA spectroscopy may be an effective method of study for various structures with 2DEG, as well as other low-dimensional systems that are in growing interest [3 – 5].

The initial expression for the absorption coefficient of photons of energy $\hbar\omega_1$ in presence (per unit volume) of photon of energy $\hbar\omega_2$ has the form [10]

$$K_2(\hbar\omega_1) = \frac{e^4}{n_1 n_2 c^2 m^4 \omega_1 \omega_2^2} \sum_{f,i} \left| \sum_t \left\{ \frac{\vec{e}_2 \vec{M}_{fi} \cdot \vec{e}_1 \vec{M}_{ti}}{E_t - E_i - \hbar\omega_1} + \frac{\vec{e}_1 \vec{M}_{ft} \cdot \vec{e}_2 \vec{M}_{ti}}{E_t - E_i - \hbar\omega_2} \right\} \right|^2 \times \delta\left[E_f - E_i - \hbar(\omega_1 + \omega_2)\right] \tag{1}$$

Here, $\vec{M}_{ft} = \langle f \left| \vec{P} \right| t \rangle$, $\vec{M}_{ti} = \langle t \left| \vec{P} \right| i \rangle$ are dipole matrix elements defined in terms of momentum operator p; e and m are the electron charge and mass; c is light velocity; $n_1$and n_2 are the index of refractions corresponding to the frequencies ω_1 and ω_2; $\vec{e}_1$, $\vec{e}_2$ are the corresponding polarizations; E_i, E_f and E_t are the energies of initial, intermediate and final states of electrons; $|i\rangle$, $|f\rangle$, $|t\rangle$ are the electronic wave functions,respectively. As follows from expression (1), the calculation of TPA coefficient is reduced to a calculation of intraband and interband matrix elements, and we must know the explicit form of wave functions and energy spectrum of electrons in the well.

2. Spectrum and wavefunctions

In Fig. 1 and energy band diagram of bulk semiconductor with degenerated valence band is shown. We shall find the carriers energy spectrum and wavefunctions in the bands using the two band Kane model with spin taken into account. We proceed from Schrödinger equation;

$$H\Psi(\vec{r}) = E\Psi(\vec{r}). \tag{2}$$

Suppose that the normal of a two dimensional surface is in z direction. Then the Hamiltonian has the form:

$$H = \frac{\vec{p}^2}{2m} + V(\vec{r}) + \frac{\hbar}{4m^2c^2}\left(\vec{\sigma} \times \vec{\nabla} V\right)\vec{p} + U(z), \tag{3}$$

where $\vec{\sigma}$ is a Pauli operator, $V\left(\vec{r}\right)$ is the periodic crystal potential, $U(z)$ is potential of a two dimensional layer.We look for solution of Eq.(2) in the form:

$$\Psi\left(\vec{r}\right)=\sum_{l} f_l\left(\vec{r}\right) u_l\left(\vec{r}\right), \tag{4}$$

where $f_l\left(\vec{r}\right)$ is a slowly changing envelope function and $u_l\left(\vec{r}\right)$ are Luttinger-Kohn amplitudes. Substituting expression (4) into (2) and taking into account (3), we have

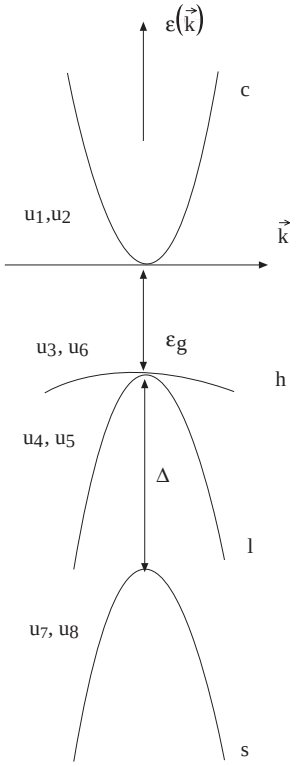

Figure 1. Band structure of $Hg_{1-x}Cd_xTe$ $(x > 0.16)$ near $\vec{k}=0$.

$$\sum_{l}\left\{\left(\frac{\vec{p}^{\,2}}{2m}+\epsilon_{l,0}-\epsilon+U\right)\delta_{l'l}+\vec{p}_{\,l'l}\,\vec{k}+\left[\frac{\hbar}{4m^2c^2}\left(\vec{\sigma}\times\vec{\nabla}\,V\right)\vec{P}\right]_{l'l}\right\} f_l\left(\vec{r}\right)=0, \tag{5}$$

where $\epsilon_{l,0}$ are the solutions of the following equation:

$$\left[\frac{\vec{p}^{\,2}}{2m}+V(\vec{r})+\frac{\hbar}{4m^2c^2}\left(\vec{\sigma}\times\vec{\nabla}\,V\right)\vec{p}\right] u_l\left(\vec{r}\right)=\epsilon_{l,0}u_l\left(\vec{r}\right). \tag{6}$$

In the above we also have:

$$u_l\left(\vec{r}+\vec{a}\right)=u_l\left(\vec{r}\right), \qquad \langle u_{l'} \mid u_l\rangle=\delta_{l'l},$$

$$\vec{p}_{l'l}=\frac{\hbar}{m}\left\langle u_{l'}\left|\vec{p}+\frac{\hbar}{4m^2c^2}\left(\vec{\sigma}\times\vec{\nabla}\,V\right)\vec{p}\right|u_l\right\rangle, \tag{7}$$

$$u_1\left(\vec{r}\right)=iS\downarrow, \qquad \epsilon_{1,0}=-\epsilon_g,$$

$$u_2\left(\vec{r}\right)=iS\uparrow, \qquad \epsilon_{1,0}=-\epsilon_g,$$

$$u_3\left(\vec{r}\right)=R_-\downarrow, \qquad \epsilon_{3,0}=0,$$

$$u_4\left(\vec{r}\right)=\sqrt{\frac{2}{3}}Z\downarrow+\sqrt{\frac{1}{3}}R_-\uparrow, \qquad \epsilon_{4,0}=0, \tag{8}$$

$$u_5\left(\vec{r}\right)=\sqrt{\frac{2}{3}}Z\uparrow+\sqrt{\frac{1}{3}}R_+\downarrow, \qquad \epsilon_{5,0}=0,$$

$$u_6\left(\vec{r}\right)=R+\uparrow, \qquad \epsilon_{6,0}=0,$$

$$u_7\left(\vec{r}\right)=\sqrt{\frac{1}{3}}Z\downarrow-\sqrt{\frac{2}{3}}R_-\uparrow, \qquad \epsilon_{7,0}=-\Delta,$$

$$u_8\left(\vec{r}\right)=\sqrt{\frac{1}{3}}Z\uparrow+\sqrt{\frac{2}{3}}R_+\downarrow, \qquad \epsilon_{7,0}=-\Delta,$$

$$R_\pm=\sqrt{\frac{1}{2}}\left(X\pm iY\right).$$

If solutions of Eq. (5) are seeked in the form $f_l=e^{i(k_xx+k_yy)}\cdot\varphi_l(z)$, then $\varphi_l(z)$ will satisfy the following equation:

$$\begin{pmatrix} H_{11} & 0 & H_{13} & H_{14} & H_{15} & 0 & H_{17} & H18 \\ 0 & H_{22} & 0 & H_{24} & H_{25} & H_{26} & H_{27} & H_{28} \\ H_{31} & 0 & H_{33} & 0 & 0 & 0 & 0 & 0 \\ H_{41} & H_{42} & 0 & H_{44} & 0 & 0 & 0 & 0 \\ H_{51} & H_{52} & 0 & 0 & H_{55} & 0 & 0 & 0 \\ 0 & H_{62} & 0 & 0 & 0 & H_{66} & 0 & 0 \\ H_{71} & H_{72} & 0 & 0 & 0 & 0 & H_{77} & 0 \\ H_{81} & H_{73} & 0 & 0 & 0 & 0 & 0 & H_{88} \end{pmatrix}\begin{pmatrix} \varphi_1 \\ \varphi_2 \\ \varphi_3 \\ \varphi_4 \\ \varphi_5 \\ \varphi_6 \\ \varphi_7 \\ \varphi_8 \end{pmatrix}=0, \tag{9}$$

where

$$\begin{array}{lll} H_{11}=-\epsilon+U(z) & H_{13}=\frac{1}{\sqrt{2}}Pk_- & H_{24}=\frac{1}{\sqrt{6}}Pk_- \\ H_{22}=-\epsilon+U(z) & H_{14}=\sqrt{\frac{2}{3}}P\overset{\wedge}{k_z} & H_{25}=\sqrt{\frac{2}{3}}P\overset{\wedge}{k_z} \\ H_{33}=-\epsilon-\epsilon_g+U(z) & H_{15}=-\frac{1}{\sqrt{6}}Pk_+ & H_{26}=\frac{1}{\sqrt{2}}Pk_+ \\ H_{44}=-\epsilon-\epsilon_g+U(z) & H_{17}=\frac{1}{\sqrt{3}}P\overset{\wedge}{k_z} & H_{27}=-\frac{1}{\sqrt{3}}Pk_- \\ H_{55}=-\epsilon-\epsilon_g+U(z) & H_{18}=\frac{1}{\sqrt{3}}Pk_+ & H_{28}=\frac{1}{\sqrt{3}}P\overset{\wedge}{k_z} \\ H_{66}=-\epsilon-\epsilon_g+U(z) & H_{ij}=(H_{ji})^* & \\ H_{77}=-\epsilon-\epsilon_g-\Delta+U(z) & \overset{\wedge}{k_z}=-i\frac{\partial}{\partial z} & \\ H_{88}=-\epsilon-\epsilon_g-\Delta+U(z) & k_\pm=k_x\pm ik_y. & \end{array} \tag{10}$$

There $P=-\frac{i\hbar}{m}\langle S\left|p_z\right|Z\rangle$ is the Kane constant, $\Delta=-\frac{3e\hbar}{4m^2c^2}\langle X\left|\frac{\partial V}{\partial x}p_y-\frac{\partial V}{\partial y}p_x\right|Y\rangle$ is the distance of split off energy band. By expressing $\varphi_3,\varphi_4,...,\varphi_8$ in terms of φ_1 and φ_2 in the last six equations and then substituting into first two equations, we have:

$$\begin{array}{c} \left\{-\epsilon+U+\frac{P^2}{3}\left[\frac{2}{\epsilon+\epsilon_g-U}+\frac{1}{\Delta+\epsilon+\epsilon_g-U}\right]\left(k_\perp^2+\overset{\wedge}{k_z^2}\right)\right. \\ \left.+\frac{P^2}{3}\left[\frac{2}{(\epsilon+\epsilon_g-U)^2}+\frac{1}{(\Delta+\epsilon+\epsilon_g-U)^2}\right]\overset{\wedge}{k_z}U\overset{\wedge}{k_z}\right\}\varphi_1+\frac{\sqrt{2}P^2k_+}{3}\left[\frac{\overset{\wedge}{k_z}U}{(\epsilon+\epsilon_g-U)^2}+\frac{\overset{\wedge}{k_z}U}{(\Delta+\epsilon+\epsilon_g-U)^2}\right]\varphi_2=0 \end{array} \tag{11}$$

$$\begin{array}{c} \left\{-\epsilon+U+\frac{P^2}{3}\left[\frac{2}{\epsilon+\epsilon_g-U}+\frac{1}{\Delta+\epsilon+\epsilon_g-U}\right]\left(k_\perp^2+\overset{\wedge}{k_z^2}\right)+\right. \\ \left.+\frac{P^2}{3}\left[\frac{2}{(\epsilon+\epsilon_g-U)^2}+\frac{1}{(\Delta+\epsilon+\epsilon_g-U)^2}\right]\overset{\wedge}{k_z}U\overset{\wedge}{k_z}\right\}\varphi_2-\frac{\sqrt{2}P^2k_-}{3}\left[\frac{\overset{\wedge}{k_z}U}{(\epsilon+\epsilon_g-U)^2}+\frac{\overset{\wedge}{k_z}U}{(\Delta+\epsilon+\epsilon_g-U)^2}\right]\varphi_1=0 \end{array} \tag{12}$$

This equation system is very complicated,therefore we shall consider the case $\Delta\to\infty$, which is also called a two-band Kane model. Then we have:

$$\begin{array}{c} \left\{-\epsilon+U+\frac{2P^2}{3}\frac{1}{\epsilon+\epsilon_g-U}\left(k_\perp^2+\overset{\wedge}{k_z^2}\right)+\frac{2P^2}{3}\frac{1}{(\epsilon+\epsilon_g-U)^2}\overset{\wedge}{k_z}U\overset{\wedge}{k_z}\right\}\varphi_1+ \\ +\frac{\sqrt{2}}{3}\frac{P^2k_+\overset{\wedge}{k_z}U}{(\epsilon+\epsilon_g-U)^2}\varphi_2=0. \end{array} \tag{13}$$

$$\begin{array}{c} \left\{-\epsilon+U+\frac{2P^2}{3}\frac{1}{\epsilon+\epsilon_g-U}\left(k_\perp^2+\overset{\wedge}{k_z^2}\right)+\frac{2P^2}{3}\frac{1}{(\epsilon+\epsilon_g-U)^2}\overset{\wedge}{k_z}U\overset{\wedge}{k_z}\right\}\varphi_2- \\ -\frac{\sqrt{2}}{3}\frac{P^2k_-\overset{\wedge}{k_z}U}{(\epsilon+\epsilon_g-U)^2}\varphi_1=0 \end{array} \tag{14}$$

In order to solve the above equation system we choose for $U(z)$ the infinitely deep square well potential:

$$U(z) = \begin{cases} \infty, & z < 0, \\ 0, & 0 \le z \le d, \\ \infty, & z > d. \end{cases} \tag{15}$$

Thus, with the potential in Eq.(15) Eqs.(13)-(14) take the form:

$$\frac{d^2\varphi_{1,2}(z)}{dz^2} + \alpha^2\varphi_{1,2}(z) = 0, \tag{16}$$

where

$$\alpha^2 = \frac{3}{2} \cdot \frac{\epsilon(\epsilon + \epsilon_g)}{P^2} - k_\perp^2. \tag{17}$$

We seek a solution of Eqs.(13)-(14) in the form:

$$\varphi_{1,2}(z) = c_1 e^{i\alpha z} + c_2 e^{-i\alpha z} \tag{18}$$

Substituting the so obtained expressions of $f_l\left(\vec{r}\right)$ into Eq. (4) we get the expression for total wave function Ψ, that contains now the constants c_1 and $c_{2.}$. From boundary conditions $\Psi(z=0)=0$ and $\Psi(z=d)=0$, we find the conditions $(1 + R_j\frac{\partial}{\partial z})\varphi_j(z = z_{bound}) = 0$ for the envelopes as in [11] . But in our case, R_j are defined by the expressions:

$$R_{j\uparrow,\downarrow} = -i \left[\frac{\sqrt{\frac{2}{3}}\frac{P}{\epsilon_j}u_4}{u_{1,2} + u_{3,6}\frac{Pk_\pm}{\sqrt{2}\epsilon_j} \mp u_{5,4}\frac{Pk_\mp}{\sqrt{6}\epsilon_j}} \right]_{z=z_{bound}}, \tag{19}$$

where the first position indices and upper signs correspond to spin up ($\uparrow$) state and second position indices together with lower signs correspond to spin down ($\downarrow$) state. We limit ourselves to the cases when the film thickness d much greater than lattice constant a_0, i.e. $d = Na_0 \gg a_0$, where N is the number of unit cells in the z direction and that the film boundaries are placed at the center of a unit cell. Then p-type amplitudes $u_{3,.....}u_6$ are equal to zero on the boundaries and $\frac{c_{1\uparrow}}{c_{2\uparrow}} = \frac{c_{1\downarrow}}{c_{2\downarrow}} = -1$.

Under the simplifications made above, for wavefunctions of light carriers we finally obtain:

$$\Psi_{\nu n_\nu \vec{k}_\perp \sigma_\nu}\left(\vec{r}\right) = \sqrt{\frac{2}{Sd}}\left\{A_{\nu n_\nu \vec{k}_\perp \sigma_\nu}\left(\vec{r}\right)\sin(\alpha_\nu z) + B_{\nu n_\nu \vec{k}_\perp \sigma_\nu}\left(\vec{r}\right)\cos(\alpha_\nu z)\right\} e^{i\vec{k}_\perp\vec{r}_\perp}. \tag{20}$$

Here, $\sigma_\nu = (\uparrow\downarrow)$, $\nu = (c,h,l)$, $k_\perp = (k_x, k_y, 0)$, and $\hat{R}=\hat{K}\cdot\hat{I}$, where $\hat{K}$ is time inversion operator and is defined as $K = -i\sigma_y K_1$ and K_1 is complex conjugating operator, $\sigma_y = \begin{pmatrix} 0 & -1 \\ 1 & 0 \end{pmatrix}$ [12].

From (17) for energy spectrum of conduction electrons and light holes we have

$$\epsilon_j = -\frac{1}{2}\epsilon_g \pm \left[\frac{1}{4}\epsilon_g^2 + \frac{2P^2}{3}\left(k_\perp^2 + \alpha_j^2\right)\right]^{\frac{1}{2}}, \alpha_j = \frac{\pi n_j}{d}, n_j = 1, 2, 3, .., \tag{21}$$

where the signs $(+)$ and $(-)$ indicate the conduction (c) and light hole (l) bands respectively and $j = c, l$.

In considered two-band model the heavy hole band doesn't interact with the other bands and therefore is parabolic:

$$\Psi_{hn_h \vec{k}_\perp \uparrow}\left(\vec{r}\right) = \sqrt{\frac{2}{Sd}}\left[\left(\frac{\sqrt{3}}{2}\frac{k_+}{k}u_4 - \frac{1}{2}\frac{k_-}{k}u_6\right)\sin\alpha_h z + \frac{i\alpha_h}{k}\frac{k_+^2}{k_\perp^2}u_3\cos\alpha_h z\right]e^{i\vec{k}_\perp \vec{r}_\perp}, \tag{22}$$

$$\Psi_{hn_h \vec{k}_\perp \downarrow}\left(\vec{r}\right) = \hat{R}\,\Psi_{hn_h \vec{k}_\perp \uparrow}\left(\vec{r}\right) \tag{23}$$

$$\epsilon_h = \frac{\hbar^2}{2m}\left(k_\perp^2 + \alpha_h^2\right), \alpha_h = \frac{\pi n_h}{d}, n_h = 1, 2, 3, ... \tag{24}$$

3. TPA calculations

In Fig. 2 the band structure of size-quantized semiconductor with degenerated valence band and all possible six TPA processes are shown in the framework of a two-band Kane model without taking spin into account. Since bands c, h and l are spin degenerated,then the number of possible processes giving contribution to TPA is equal to 48. If one takes into account that the matrix elements between spin up and spin down states within the same band are zero, $\langle c\ \vec{k}\uparrow|\vec{e}\vec{p}|\ c\ \vec{k}\downarrow\rangle = \langle h\ \vec{k}\uparrow|\vec{e}\vec{p}|\ h\ \vec{k}\downarrow\rangle = \langle l\ \vec{k}\uparrow|\vec{e}\vec{p}|\ l\ \vec{k}\downarrow\rangle$, and if one neglects the matrix elements $\left\langle h\ \vec{k}\uparrow|\vec{e}\vec{p}|\ h\ \vec{k}\uparrow\right\rangle = \langle h\ \vec{k}\downarrow|\vec{e}\vec{p}|\ h\ \vec{k}\downarrow\rangle$ as might be allowed by of the small parameter (m_l/m_h), then the number of TPA processes are reduced to 28. By taking all these circumstances into account, TPA coefficient for small gap semiconductors of type InSb was calculated in $[13-14]$ for bulk case and nonparabolic electron spectrum for arbitrary $\vec{k}$.

We have calculated the TPA coefficient for size-quantized semiconductor films with degenerated valence band. In the presence of the size-quantized states, a number of TPA processes are drastically increased due to the additional interband (intersubband transitions between the different bands) and intraband (intersubband transitions within one band) transitions both for $\Delta n = 0$ and $\Delta n \neq 0$ cases, where $\Delta n = n_f - n_i$ are subband number differences. In contrast to the bulk case, in size quantized structures the transitions between the spin up and spin down states are possible for processes with $\Delta n \neq 0$. For simplicity, consider the parabolic case. In Fig. 2 four processes corresponding to two photon transitions from the valence subband to conduction subband are shown, when the intermediate states are the conduction band subbands. If one takes into account that valence band subbands are also involved in intermediate states then the total number

of possible TPA processes increases by two.

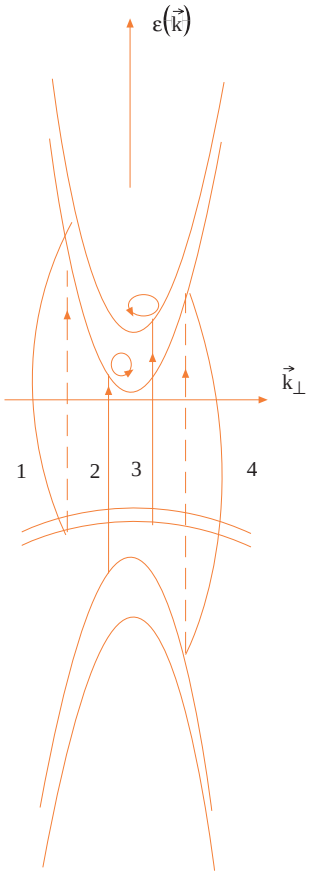

Figure 2. Band structure of size-quantized semiconductor $Hg_{1-x}Cd_xTe$ with $x > 0.16$ and possible TPA processes.

Intraband and interband matrix elements have been calculated in [15 – 18]. However, the explicit form of wave functions, i.e. the dependencies of Bloch factors $u_{n_\nu \vec{k}_\perp}\left(\vec{r}\right)$ on wave vector $\vec{k}_\perp$ and subband number n_ν, were not taken into account. Yet, the optical properties of size-quantized films are very sensitive to the geometry of the experiment and therefore it is vital to consider the explicit form of Bloch factors.

As a result of tedious calculations for the TPA coefficient we obtain the following expression:

$$K_2(\hbar\omega) = \frac{8\pi^2 e^4 P^2}{n_1 n_2 c^2 \hbar d} \sum \left(\frac{m_{cj}}{m_c}\right)^2 \sum\sum f_{ij}(\omega_1, \omega_2) \frac{\Theta(\Lambda_{cj})}{\hbar\omega_1 (\hbar\omega_2)^2}, \tag{25}$$

where $f_{ji}(\omega_1,\omega_2)$ for zz and "++" polarizations has the form:

$$\begin{array}{c} .f_{h1}^{zz}=0, \\ f_{h2}^{zz}=\frac{\epsilon_{ch}^{0}}{\pi^2}\xi_{1hh}^{2}\left(a_{ha_h}^{cn_h}+b_{ha_h}^{cn_h}\right)^2\left|T_{n_cn_h}\right|^2, \\ f_{h3}^{zz}=0, \end{array} \tag{26}$$

$$\begin{array}{c} f_{l1}^{zz}=0, \\ f_{l2}^{zz}=\frac{\epsilon_{cl}^{0}}{3\pi^2}\left[\xi_{1ll}(a_{\ln_l}^{cn_l}+b_{\ln_l}^{cn_l})+\xi_{1lc}(a_{\ln_l}^{\ln_c}+b^{\ln_c})\right]^2\left|T_{n_cn_l}\right|^2, \\ f_{l3}^{zz}=\frac{4\epsilon_{cl}^{0}}{3\pi^2}\left[\sum\limits_{n_c^{'}}\xi_{2ll}\cdot T_{n_cn_c^{'}}\cdot T_{n_c^{'}n_l}\cdot(a_{\ln_l}^{cn_c^{'}}+b_{\ln_l}^{cn_c})+\sum\limits_{n_l^{'}}\xi_{2ll}\cdot T_{n_cn_l^{'}}\cdot T_{n_l^{'}n_c}(a_{\ln_l}^{\ln_l^{'}}+b_{\ln_l}^{\ln_l^{'}})\right]^2, \end{array} \tag{27}$$

$$\begin{array}{c} f_{h1}^{++}=\frac{1}{2}\Lambda_{ch}\xi_{1hh}^{2}\cdot\left(a_{hn_h}^{cn_c}+b_{hn_h}^{cn_c}\right)^2\delta_{n_cn_h}, \\ f_{h2}^{++}=\frac{1}{2}\Lambda_{ch}\xi_{2hh}^{2}\cdot\left(a_{hn_h}^{cn_c}+b_{hn_h}^{cn_c}\right)^2\cdot\left|T_{n_cn_h}\right|^2, \\ f_{h3}^{++}=0, \end{array} \tag{28}$$

$$\begin{array}{c} f_{l1}^{++}=\frac{5}{12}\Lambda_{cl}\xi_{1ll}^{2}\cdot\left(a_{\ln_l}^{cn_c}+b_{\ln_l}^{cn_c}+a_{\ln_l}^{\ln_l}+b_{\ln_l}^{\ln_l}\right)^2\cdot\delta_{n_cn_l}, \\ f_{l2}^{++}=\frac{1}{6}\Lambda_{cl}\xi_{2ll}^{2}\cdot\left(a_{\ln_l}^{cn_c}+b_{\ln l}^{cn_c}+a_{\ln_l}^{\ln_l}+b_{\ln_l}^{\ln_l}\right)^2\cdot\left|T_{n_cn_l}\right|^2, \\ f_{13}^{zz}=0, \end{array} \tag{29}$$

$$\epsilon_{cj}^{0}=\epsilon_{c}^{0}+\epsilon_{j}^{0},\Lambda_{cj}=\hbar\left(\omega_1+\omega_2\right)-\epsilon_g-\epsilon_{c}^{0}n_c^2-\epsilon_{j}^{0}n_j^2, \tag{30}$$

$$\xi_{1j\nu}=\frac{\Lambda_{cj}}{\Lambda_{cj}+\epsilon_{cj}n_\nu^2},\xi_{2j\nu}=\frac{1}{\pi^2}\frac{\epsilon_{cj}}{\Lambda_{cj}+\epsilon_{cj}n_\nu^2}, \tag{31}$$

$$a_{jn_j}^{cn_\nu}=\left[\hbar\omega_1+\epsilon_{c}^{0}(n_\nu^2-n_j^2)\right]^{-1},b_{jn_j}^{cn_\nu}=a_{jnj}^{cn_\nu}\cdot\delta_{\omega_1\omega_2}, \tag{32}$$

$$a_{\ln_l}^{\ln_\nu}=\left[-\hbar\omega_2-\epsilon_{l}^{0}(n_\nu^2-n_l^2)\right]^{-1},b_{\ln_l}^{\ln_\nu}=a_{\ln_l}^{\ln_\nu}\cdot\delta_{\omega_1\omega_2}, \tag{33}$$

$$\Theta(x)=\left\{\begin{smallmatrix}1,x\geq0\\0\ ,x<0\end{smallmatrix}\right\},\delta_{ij}=\left\{\begin{smallmatrix}1,i=j\\0\ ,i\neq j\end{smallmatrix}\right\},\begin{smallmatrix}\nu=(c\ ,\ j)\\j=(h\ ,l)\end{smallmatrix}, \tag{34}$$

$$\frac{1}{m_{cj}}=\frac{1}{m_c}+\frac{1}{m_j};T_{n_cn_j}=\left[1-(-1)^{n_c+n_j}\right]\cdot\frac{2n_cn_j}{n_c^2-n_j^2}. \tag{35}$$

In Fig. 3 the dependencies of TPA coefficient K_2 on the parameter $\hbar\omega/\epsilon_g$ with $\omega_1=\omega_2=\omega$, as calculated from Eq.(25) for geometries zz and "++" for $d=400\mathring{A}$ and $\epsilon_g=0.31eV$, $m_h=0.4m_0$, $m_l=\left(3\hbar^2\epsilon_g\right)/\left(4P^2\right)$, $P=8\cdot10^{-8}eV\cdot cm$ are shown. The continuous curve corresponds to zz geometry and the dashed curve corresponds to "++"

geometry. Arrows indicate transitions to conduction band from heavy hole subbands (1-1$h \rightarrow 1c$, 2-2$h \rightarrow 1c$, 3-1$h \rightarrow 2c$ and 5-2$h \rightarrow 3c$) and from light hole subbands (4-2$l \rightarrow 1c$ or $1l \rightarrow 2c$ and 6-3$l \rightarrow 2c$ or $2l \rightarrow 3c$). As follows from the figure for the zz geometry case the size quantization is clearly exhibited in TPA spectrum. TPA begins from threshold that corresponds to the energy difference between first conduction band subband and second heavy hole subband, shown as arrow 2. The other arrows indicate transitions with selection rules $\Delta n_{cj} = n_c - n_j = 2k + 1 (k = 0, \pm 1, \pm 2, ...)$, where $j = (h, l)$, i.e. 3-1$h \rightarrow 2c$, 4-2$l \rightarrow 1c$ or $1l - 2c$, 5-2$h \rightarrow 3c$ and 6-3$l \rightarrow 2c$ or $2l \rightarrow 3c$. As also seen from the figure for "++" geometry, the size levels do not appear. This is associated with the fact that, in this case the main contribution comes from transitions with $\Delta n_{cj} = 0$. Looking at expressions $(26) - (29)$ we see that for "++" geometry there is also possible the transitions with selection rule $\Delta n_{cj} = 2k + 1$ $(k = 0, \pm 1, \pm 2, ..)$; however their contribution is considerably small.

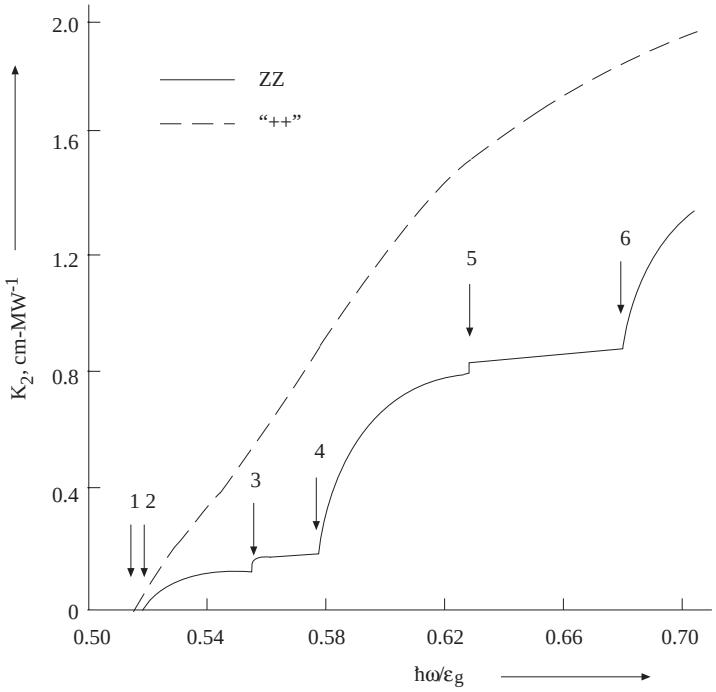

Figure 3. Dependence of TPA coefficient on the parameter $\hbar\omega/\epsilon_g$ with $\omega_1 = \omega_2 = \omega$ for $d = 400 \overset{o}{A}$ and $\epsilon_g = 0.31eV$.

Fig.4 shows the TPA coefficient K_2 versus $\hbar\omega/\epsilon_g$ for two different thicknesses. It follows that, with decreasing thickness the energetic distances, between size subbands increase and TPA spectrum shifts toward short waves.

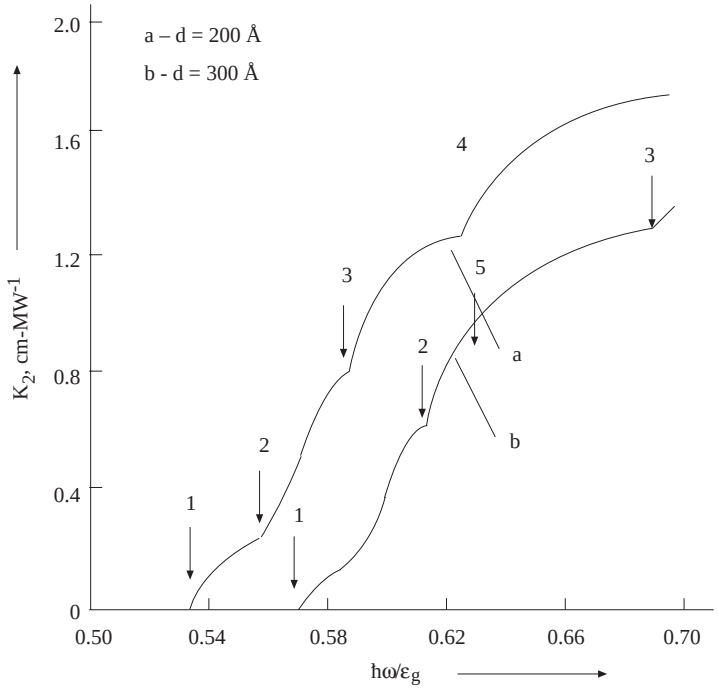

Figure 4. TPA coefficient K_2 versus $\hbar\omega/\epsilon_g$ for ZZ geometry for different thicknesses.

Fig. 5 shows $\hbar\omega/\epsilon_g$ dependence of K_2 for the same parameters as used in Fig.3 for $d = 200\mathring{A}$ in the case of "++" geometry with selection rule $\Delta n_{cj} = 2k+1$. The threshold corresponds to $2h \rightarrow 1c$ transition, which is shown by arrow 1. Arrow 2 indicates the transitions $3h \rightarrow 1c$, $3h \rightarrow 1h$, and 4-$3h \rightarrow 2c$.

4. Concluding remarks

In the framework of the two-band Kane's model we have carried out a detailed investigation of TPA of light by two-dimensional electron gas which can be realized in various structures on the basis of semiconductors with the degenerated valence band. The calculations are made for a thin film of semiconductors of type of $GaAs$, $InSb$, $HgCdTe$, $HgMnTe$.

The general formula for TPA coefficient K_2 is obtained with taking into account all the possible two-photon processes allowed by this model. The formula involves also the all possible polarizations of incident photons.

It is stated that K_2 is essentially determined by dependences of Bloch factors on the electron wave vector. The values of K_2 in various geometries differ from each other by ∼20-40%. In ZZ geometry the TPA coefficient K_2 as a function of frequency has an step-like behavior, but for $(++)$ geometry K_2 is monotonic.

It is shown that in addition to processes with selection rule $\Delta n = 0$, the processes

with $\Delta n = \pm 1, \pm 3, \pm 5, ...$ take place. The values of K_2 for these processes are smaller approximately by two order than that of $\Delta n = 0$.

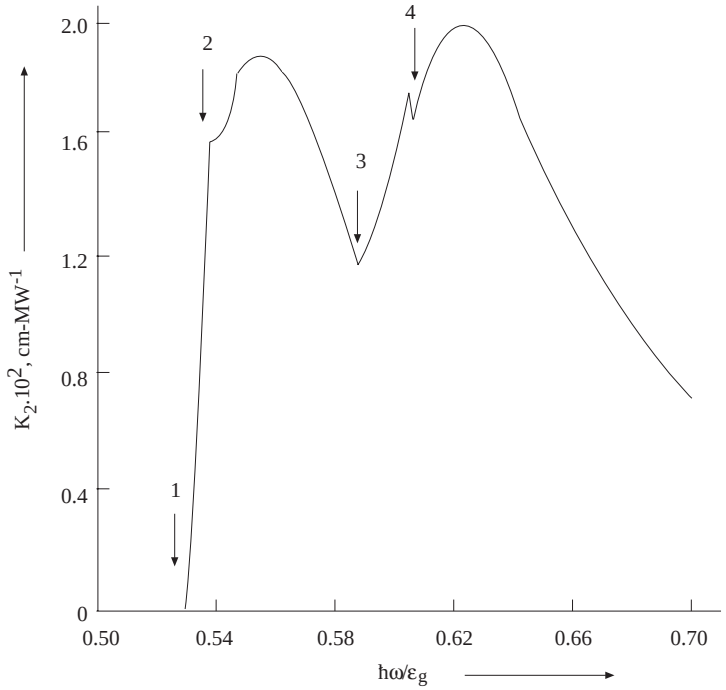

Figure 5. TPA coefficient with selection rules $\Delta n = \pm 1, \pm 3, ...$ for " $+ +$" geometry for $\epsilon_g = 0.31eV$ and $d = 200 \overset{o}{A}$.

Acknowledgments

One of the authors (T.G.I.) wishes to thank the Scientific and Technical Research Council of Turkey (TUBITAK) for hospitality and financial support during his visit to Ankara University.

References

[1] Zh. Alferov. Semiconductors, 32 (1), 1 (1998).

[2] Hiroshi Okamoto. Jap. Journ. of Appl. Phys., 26 (3), 315 (1987).

[3] D.A. Ioffe. Advances in Physics, 42 (2), 173 (1993).

[4] C.R. Pidgeon, C.M. Ciesla, B.N. Murdin. Prog. Quant. Electr., 21 (5) 361 (1998).

[5] S.V. Gaponenko. Fizika i Texnika Poluprovodnikov, 30 (2), 577 (1996).

[6] M.S. Brodin,V.Ya. Reznichenko. Interaction of high intensity laser radiation with semiconductors A^2B^6//In book: Fizika soedineniy A^2B^6.-M. Nauka, 1986.-p.184-225.

[7] N.G. Basov, A.Z. Grasyuk, I.G. Zubarev, V.A. Katulin. Fiz.Tv.Tela,7(12), 3639(1965).

[8] N.G. Basov, A.Z. Grasyuk, I.G. Zubarev, V.A. Katulin, O.N. Krokhin. Zh. Eksp. Teor. Fiz. 50 (3), 551 (1966).

[9] A.Z. Grasyuk, I.G. Zubarev, A.N. Mentser. Fiz. Tv. Tela, 10 (2), 543 (1968).

[10] A.M. Johnston, C.R. Pidgeon, Dempsey. Phys. Rev. B22 (22), 825 (1980).

[11] V.A. Volkov, T.N. Pinsker. Zh. Eksp. Teor. Fiz. 70, 2268 (1976).

[12] C. Kittel. Quantum Theory of Solids, New-York-London (1963).

[13] A.M. Johnston, C.R. Pidgeon, J. Dempsey. Phys. Rev. B22 (22), 825 (1980).

[14] M.H. Weiler. Solid St. Comm., 39, 937 (1981).

[15] V.V. Sokolov. Izv. visshikh ucheb. zav., XVIII (2), 207(1975).

[16] V.D. Prodan, Ya. A. Rozneritsa. Fiz. Tekhn. Polupr., 9(1), 145 (1975).

[17] M. Zaluzny. Thin Solid Films, 55, 243 (1978).

[18] N.N. Spector. Phys. Rev. B35(11), 5876 (1987).